JETP Letters, Vol. 81, No. 10, 2005, pp. 491–493. Translated from Pis'ma v Zhurnal Éksperimental'noĭ i Teoreticheskoĭ Fiziki, Vol. 81, No. 10, 2005, pp. 610–613.

Tunneling of X-ray Photons through a Thin Film under Total Internal Reflection Conditions

A. G. Touriyanskiĭ and I. V. Pirshin

Lebedev Physical Institute, Russian Academy of Sciences, Leninskiĭ pr. 53, Moscow, 119991 Russia

e-mail: tour@mail1.lebedev.ru

Received April 22, 2005

Tunneling of 0.154- and 0.139-nm x-ray photons through a thin film under total internal reflection conditions has been experimentally demonstrated. The $NiSi_2$ film 13 nm thick is deposited by magnetron sputtering on a polished Si substrate. A beam with an angular spread of 20″ is directed to the $Si/NiSi_2$ interface from the inside through the lateral surface of a sample. A peak associated with tunneling of photons from Si to air through the $NiSi_2$ film is observed at grazing angles of $\theta_1 > 0.4\theta_c$, where θ_c is the critical angle of total internal reflection at the $Si/NiSi_2$ interface. The integral intensity of tunneling peaks that is measured for various θ_1 angles agrees with the calculations. © *2005 Pleiades Publishing, Inc.*

PACS numbers: 07.60.Hv, 07.85.Fv, 41.50.+h

The phenomenon of frustrated total internal reflection is well known in optics [1, 2]. The passage of radiation through a thin gap with an optically less dense medium under the formal conditions of total internal reflection is usually treated as tunneling of photons through an optical barrier. The effective wave-penetration depth z_e for grazing angles θ_1 smaller than the critical angle θ_c of total internal reflection depends on the incident radiation wavelength λ and the environment parameters. For this reason, frustrated total internal reflection in optical and IR spectral ranges is widely used at present to analyze the composition and structure of thin films and interfaces [3–5]. For hard x-ray radiation with $\lambda \sim 0.1$ nm, the refractive index decrement $\delta = 1 - n$ (n is the refractive index) for most materials lies in the range 10^{-6}–10^{-5}. For these δ values, total internal reflection can be observed only in a very narrow angular range. According to calculations and experimental data [6], the typical z_e values are 2–3 nm, which are less than one hundredth of the typical z_e values for the optical range.

Therefore, the direct observation of frustrated total internal reflection in the x-ray range is of fundamental and practical interest. In this work, we show that the effect can be detected under laboratory conditions and present the results of measurements of the angular distribution of the intensity of x-ray photon tunneling from silicon to air through the $NiSi_2$ thin film.

An optically polished Si single crystal disk was used as a substrate. The $NiSi_2$ film was deposited by the magnetotron sputtering. The film was partially oxidized due to interaction with air. According to x-ray reflectometry, the thickness of the nonoxidized $NiSi_2$ film was equal to 12.8 nm. A plate 1-cm wide was made from the central part of the disk by scribing from the side opposite to the film and subsequent splitting.

Measurements were carried out by means of an x-ray reflectometer whose x-ray optical scheme was described in [7]. A sharp focus x-ray tube with a copper anode was used as a radiation source. Figure 1 shows the position of a sample with respect to the incident radiation. A beam with an angular spread of 20″ was directed through the lateral surface of the sample. The edge of the lateral face of the sample was aligned with the reflectometer rotation axis. Thus, the flux density of the x-ray radiation incident on the lateral face remained constant under small rotations. The angular distribution of the intensity $I(\psi)$ of radiation passed through the sample at fixed grazing angles θ_1 of the primary beam was measured by scanning by a receiving slit that had a width s of 30 or 100 μm and was situated at a distance

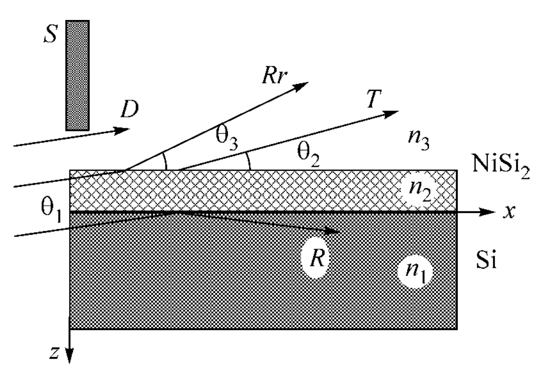

Fig. 1. Radiation passage scheme: (S) protection screen, (D) direct beam at grazing angle θ_1, (Rr) refracted beam at grazing angle θ_3, (R) reflected beam, and (T) beam tunneling through $NiSi_2$ at grazing angle θ_2.

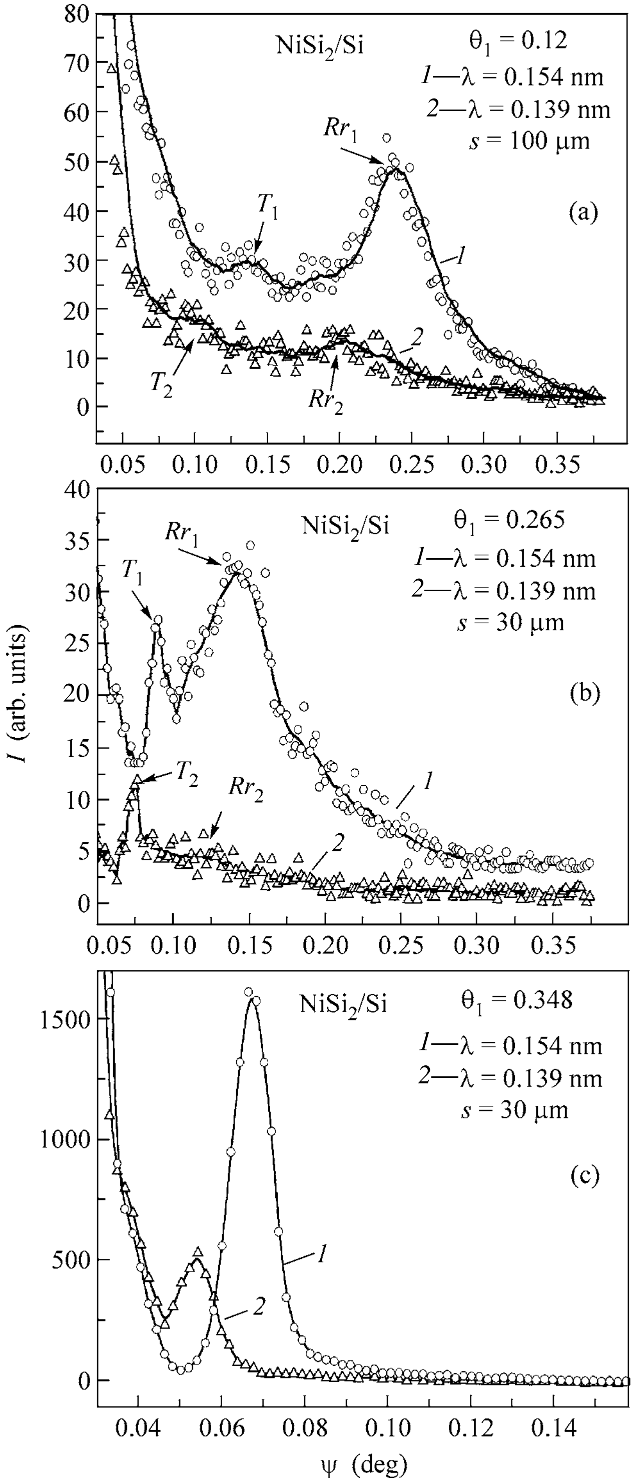

Fig. 2. Angular distributions of the intensity of the radiation passed through the sample for the grazing angles of the primary beam θ_1 = (a) 0.12°, (b) 0.265°, and (c) 0.348° and for (*1*) CuK_α 0.154-nm and (*2*) CuK_β 0.139-nm lines; panels (a) and (b) correspond to the tunneling regions and panel (c), to the reflection region.

of 225 mm from the reflectometer axis. The deviation angle ψ of radiation passed through the sample was measured from the primary beam axis. The spectral lines CuK_α (0.154 nm) and CuK_β (0.139 nm) were separated by semitransparent monochromators from radiation passed through the receiving slit. The angular scanning step and the direct radiation flux at the CuK_α line were equal to 3.6″ and 10^6 photons per second, respectively.

For the measurement geometry shown in Fig. 1, a certain part of the beam passed between the absorbing screen S and sample surface and was used as an angular reference. Another part of the beam passed through the lateral surface of the film and was refracted at the $NiSi_2$/air interface at the grazing angle θ_3. The main part of the beam entering the substrate was absorbed in Si. Photons whose path in Si is smaller than the mean free path l_s of x-ray photons predominantly reach the Si/$NiSi_2$ interface. The mean free path l_s for the CuK_α and CuK_β lines is equal to 71 and 99 μm, respectively. According to the table data [8], $\delta(\text{Si}) = 7.57 \times 10^{-6}$ and $\delta(\text{NiSi}_2) = 21.5 \times 10^{-6}$ for $\lambda = 0.154$ nm; i.e., the necessary condition of the total internal reflection $1 - \delta(\text{Si}) > 1 - \delta(\text{NiSi}_2)$ is satisfied at the Si/$NiSi_2$ interface. Thus, this part of the x-ray flux can tunnel from Si to air through the $NiSi_2$ film.

The condition of the passage of the wave front through the lateral surface of the substrate without significant distortion can be written in the form

$$\Delta L(n_3 - n_1)/\lambda = \Delta L\delta(\text{Si})/\lambda \ll 1, \qquad (1)$$

where ΔL is the mean height of ribs on the chip surface. Substituting the table δ value for Si at $\lambda = 0.154$ nm and, for definiteness, assuming that the left-hand side of the inequality is no more than 0.01, we obtain $\Delta L < 0.2$ μm. The above condition is easily satisfied on the chips of the single crystal along the cleavage planes within sections that are much larger than the diameter of the first Fresnel zone.

Figure 2 shows the measured angular distributions of the intensity $I(\psi)$ of radiation passed through the sample at fixed grazing angles θ_1 of the primary beam. As was mentioned above, a sharp increase in the intensity for angles $\psi \longrightarrow 0$ is associated with the passage of a part of the direct beam over the sample edge. As follows from the geometry of the radiation, the broad peak on the right side of Figs. 2a and 2b arises due to the refraction of x-ray radiation passed through the end of the $NiSi_2$ film. The corresponding refraction maxima are denoted as Rr_1 and Rr_2. In the diagram measured on the CuK_β line, the Rr_2 peak is lower than the background signal, which is caused by the jump in the photoabsorption in Ni for $\lambda = 0.139$ nm. The tunneling flux can be measured beginning with the grazing angle $\theta_1 = 0.12°$ (Fig. 2a). The tunneling peaks for the two wavelengths in Figs. 2a and 2b are denoted as T_1 and T_2. For grazing angles $\theta_1 > \theta_c$ (Fig. 2c), only the intense peak of refracted radiation passing from silicon to air through the Si/film and film/air interfaces is observed.

Figure 3 shows (*1*) experimental and (*2*) theoretical dependences of the integral intensity Φ of x-ray radiation passed through the film at the grazing angle θ_1 for $\lambda = 0.154$ nm. The function Φ values are obtained by numerically integrating the $I(\psi)$ curve near the tunneling peak and subtracting the background signal. The angular range $\theta_1 < \theta_c \approx 0.31°$ is the tunneling region.

The angular dependence $\Phi(\theta_1)$ is calculated under the following assumptions. We assume that the angular spread of the primary beam is negligible and the linear flux density p_0 of x-ray photons incident on the end of the sample at the grazing angle θ_1 is constant. The z axis is perpendicular to the sample surface (see Fig. 1). In this case,

$$\Phi(\theta_1) = |t_1|^2 \int_0^\infty p_0 \exp\left(-\frac{\mu(z)z}{\sin\theta_1}\right) dz, \quad (2)$$

where p_0 is the linear density of the x-ray flux incident on the sample and μ is the linear coefficient of the absorption of radiation in the substrate for the given wavelength. The energy transmission coefficient $T = |t_1|^2$ of the film structure is calculated from the recurrence relations [9]

$$t_j = \frac{t_{j+1} t_j^{\mathrm{F}} e^{i\kappa_2 d_j}}{1 + r_{j+1} r_j^{\mathrm{F}} e^{2i\kappa_2 d_j}}, \quad (3)$$

$$r_j = \frac{r_j^{\mathrm{F}} r_{j+1} e^{2i\kappa_{j+1} d_j}}{1 + r_{j+1} r_j^{\mathrm{F}} e^{2i\kappa_{j+1} d_j}}. \quad (4)$$

Here, r_j and t_j are the complex amplitude coefficients of reflection and transmission of the structure, respectively; r_j^{F} and t_j^{F} are the Fresnel amplitude coefficients of reflection and transmission at the interfaces, respectively; $\kappa = 2\pi/\lambda(\varepsilon_j - \sin^2\varphi)^{1/2}$, where $\varphi = \pi/2 - \theta_1$ is the angle of incidence on the first interface and ε_j is the dielectric constant of the medium in the jth layer; and d_j is the layer thickness.

Comparison shows that the experimental and theoretical curves are in fairly good agreement. The result shown in Fig. 3 is obtained with the effective film thickness $D_f = 18.5$ nm, which testifies to the presence of an oxide layer. This conclusion is also corroborated by x-ray reflectometry. For grazing angles $\theta_1 < 0.7\theta_c$, the tunneling photon flux is lower than 1% of the reflected flux for $\theta_1 \approx 1.1\theta_c$. The conditional boundary between the regions of tunneling and refraction is shown in Fig. 3 by the vertical dashed straight line. The presence of the extended transient section on the curve $\Phi(\theta_1)$ in the region $\theta_1 \approx \theta_c$ is explained by the effect of the imaginary part of ε.

In conclusion, we note that, for such materials as GaAs, Al_2O_3, Si, and fused silica that are most often used as substrates, the mean free path of photons for $\lambda = 0.154$ nm and, correspondingly, the effective width of the tunneling region are in the range 30–140 μm. These values are approximately two orders of magnitude smaller than the characteristic size of the irradiated region in x-ray reflectometry measurements. For this reason, the transmission measurement scheme proposed in this work can be used to analyze edge effects in the technology of producing film nanostructures and to control coatings on a nonflat surface with a curvature radius to 0.3–0.5 m.

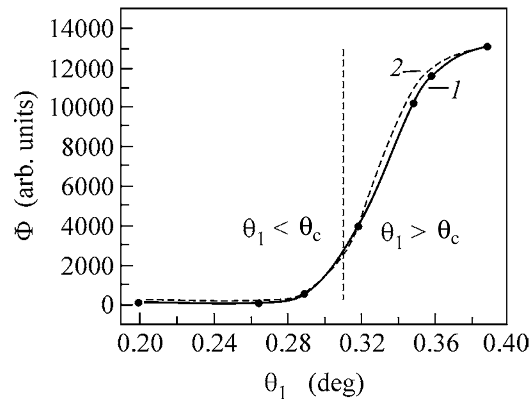

Fig. 3. (*1*) Experimental and (*2*) theoretical angular dependences of the integral flux intensity of x-ray photons passed through the outer interface: $\theta_1 < \theta_c$ is the tunneling region and $\theta_1 > \theta_c$ is the refraction region.

We are grateful to N.N. Gerasimenko for samples placed at our disposal. This work was supported in part by the Russian Foundation for Basic Research, project no. 03-02-16976a.

REFERENCES

1. C. Hirlimann, B. Thomas, and D. Boosé, Europhys. Lett. **69**, 48 (2005).
2. J. J. Carey, J. Zawadzka, D. A. Jaroszynski, *et al.*, Phys. Rev. Lett. **84**, 1431 (2000).
3. D. C. Beddows, B. C. Griffiths, O. Samek, *et al.*, Appl. Opt. **42**, 6006 (2003).
4. A. A. Golubtsov, N. F. Pilipetskiĭ, A. N. Sudarkin, *et al.*, Pis'ma Zh. Éksp. Teor. Fiz. **43**, 219 (1986) [JETP Lett. **43**, 277 (1986)].
5. Yu. I. Malakhov, A. L. Kalabekov, and Yu. N. Korolev, Izmer. Tekh., No. 8, 40 (2002).
6. K. Sakurai, *X-Ray Spectrometry: Recent Technological Advances*, Ed. by K. Tsuji, J. Injuk, and R. Van Grieken (Wiley, Chichester, 2004).
7. A. G. Tur'yanskiĭ, A. V. Vinogradov, and I. V. Pirshin, Prib. Tekh. Éksp., No. 1, 105 (1999).
8. B. L. Henke, E. M. Gullikson, and J. C. Davis, At. Data Nucl. Data Tables **54**, 181 (1993).
9. P. H. Berning, in *Physics of Thin Films*, Ed. by G. Haas (Academic, New York, 1963), Vol. 1, p. 69 [P. H. Berning, *Theory and Calculations of Optical Thin Films* (Mir, Moscow, 1967), Vol. 1].

Translated by R. Tyapaev